Third International Symposium on Marine Propulsors
smp'13, Launceston, Tasmania, Australia, May 2013

On the Propulsive Efficiency of Unsteady Propulsors

Michael Krieg[1,3], **Kamran Mohseni**[1,2,3]

[1]Department of Mechanical and Aerospace Engineering,
[2]Department of Computer and Electrical Engineering,
[3]Institute for Networked Autonomous systems, University of Florida, Gainesville, Florida

ABSTRACT

This study examines the propulsive efficiency of underwater vehicles which are driven by unsteady propulsors. The analysis is focused on vehicles utilizing a novel thruster which expels finite propulsive jets periodically. This analysis also applies to swimming squid and jellyfish (from which the thruster was inspired), and can also be extended to any periodic unsteady propulsion. The vehicle trajectory is solved analytically to calculate the exact work output/input and it is observed that with unbounded forcing there is an optimal thruster duty cycle, $\lambda = 0.31$, which maximizes propulsive efficiency. This optimal duty cycle is very close to the actual jetting duty cycle observed in steadily swimming squid.

Keywords

Pulsed Jet, Biomimicry, Vortex Formation, Radial Velocity.

1 INTRODUCTION

A vehicle with a high propulsive efficiency is clearly advantageous in almost any application, but the large spacial scales and lack of support infrastructure in marine environments makes propulsive efficiency a critical factor for underwater vehicles. Propulsive efficiency is the ratio of the useful propulsive work done on a vehicle to the total energy required to generate the propulsion. Useful propulsive work is defined as the integral of propulsive force applied to the vehicle over the vehicle trajectory, which is often approximated as the product of propulsive force and total distance traveled for steady propulsion mechanisms.

Traditional propulsive efficiency analysis led multiple researchers to the conclusion that low volume high velocity propulsive jets inherently negate a high propulsive efficiency Alexander (1968); Lighthill (1975); Vogel (2003); however, empirical testing which determines propulsive efficiency from PIV analysis of the wake behind swimming squid has shown that certain species have rather high propulsive efficiency, averaging $69\% \pm 14\%$ over multiple species and a range of swimming speeds Bartol et al. (2009), and in some cases even rivaling propulsive efficiencies of nature's long distance swimmers 78% for adult *L. brevis* and $87\% \pm 6.5\%$ for paralarvae *L. brevis* Bartol et al. (2008).

A new type of thruster has been developed for use on underwater vehicles which is inspired by the locomotion of squid and other cephalopods Mohseni (2004, 2006). This thruster generates propulsive forces by successively ingesting and expelling jets of water from a cavity internal to the vehicle hull, with only a small orifice exposed to the external flow. This type of thruster is advantageous because it provides the vehicle with propulsive forces necessary for accurate low speed maneuvering while maintaining a low forward drag profile, which is necessary for efficient long range transit. Furthermore, the thrust is generated nearly instantaneously Krieg & Mohseni (2010) unlike propeller thrusters Yoerger et al. (1990); Fossen (1991) and tunnel thrusters Mclean (1991). The feasibility of this type of maneuvering system has been verified by several generations of vehicles equipped with the thrusters shown in Figure 1 Mohseni (2006); Clark et al. (2009); Krieg & Mohseni (2010); Krieg et al. (2011). All of these thruster iterations generate fluid motion by actuating a flat plunger (or piston) within the thruster cavity.

However, the propulsive efficiency of unsteady periodic thrusting must be clarified before this technology can become commonplace.

This paper examines an unsteady propulsor which can be described by periodic alternation between binary states (either on or off) with a given duty-cycle, acting on an underwater vehicle which travels in a single direction. After some time the vehicle comes to a quasi-equilibrium state with a steady average velocity (actual velocity oscillates around this average). The vehicle trajectory is solved analytically in Section 2, and the useful propulsive work done over this trajectory as well as the total energy required to drive the thruster are calculated in Section 3. Section 4 presents the results of the propulsive efficiency calculations, and identifies optimal thruster duty cycles.

2 QUASI-STEADY VEHICLE TRAJECTORY

Any underwater vehicle which is subject to periodic constant forcing will experience an acceleration during the time when the forcing is on, and a deceleration due to drag forces during the time when the forcing is off. When the

Figure 1: Progression of squid inspired thrusters developed for vehicle propulsion, moving from oldest to most recent (a) initial design Mohseni (2004), (b) first successful vehicle design Krieg et al. (2005), (c) improved capacity Clark et al. (2009), (d) most recent design has simple and reliable driving mechanism Krieg et al. (2011).

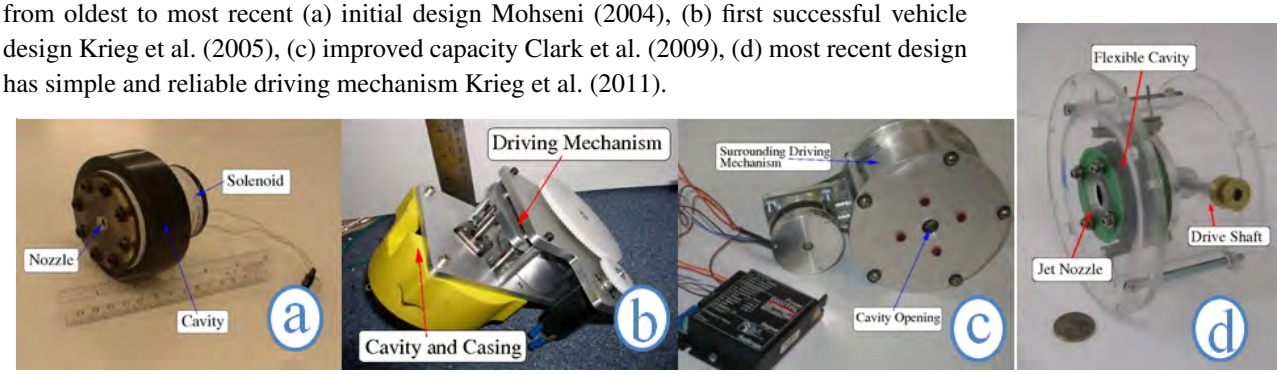

vehicle is first accelerated from rest there is much more acceleration than deceleration and the average velocity over the forcing cycle will increase from cycle to cycle. After some time the average velocity becomes high enough that the deceleration phase becomes equivalent to the acceleration phase, and the average velocity remains constant during all subsequent forcing cycles. We will refer to this as a 'quasi-equilibrium' state because the average vehicle velocity has reached equilibrium despite the continual oscillation in vehicle velocity over the cycle. As the most simple case consider a vehicle which consists of a cylinder which is forced and moves in a single direction, x, orthogonal to its axis of symmetry, as is depicted in Figure 2. The equation of motion for this vehicle is just newton's second law including both thruster and drag forces,

$$m\ddot{x} = F(t) + F_{\text{drag}}\,, \quad \textit{and} \quad F_{\text{drag}} = -\frac{1}{2}\rho S C_D \dot{x}\,|\dot{x}|\,. \tag{1}$$

Here F is the thruster force, F_{drag} is the drag force, ρ is the density of the fluid medium, S is the wetted area of the vehicle, and C_D is the drag coefficient. The drag coefficient is a function of Reynolds number, $Re = \dot{x}\nu/d_s$, which is well known for a cylinder in cross flow, and can be approximated as a constant for high Re flow or inversely proportional to Re for low Re flow.

$$C_D \approx \begin{cases} 0.81 & : \text{ High } Re \\ \frac{10\nu}{d\dot{x}} & : \text{ Low } Re \end{cases} \tag{2}$$

Though the shape of the vehicle is chosen to be a cylinder for simplicity, it is actually a decent representation of the vehicle since the thrusters of this study provide maneuvering forces without compromising the streamlined shape of the vehicle, as is shown in Figure 3.

2.1 Thruster Force

This investigation is focused on a new type of thruster which is inspired by the locomotion of squid and jellyfish. The nature of the propulsive jet, and consequently the thrust output, is observed to depend greatly on the nozzle configuration partially due to the resulting radial velocity

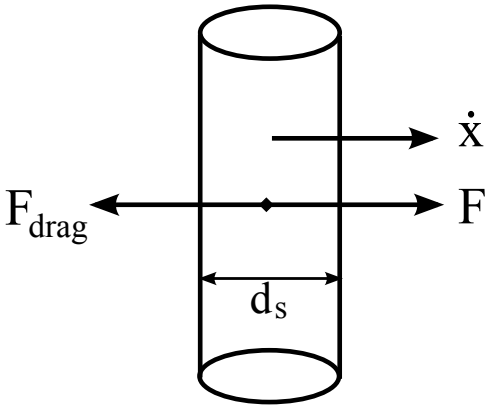

Figure 2: Hypothetical vehicle with one degree of freedom (in the x direction).

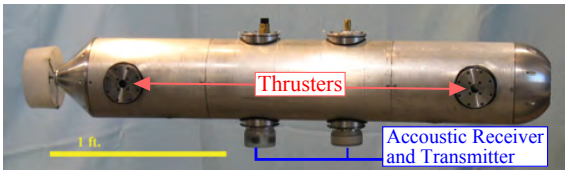

Figure 3: The most recent vehicle to be developed using squid inspired thrusters at the University of Florida, described in great detail in Krieg et al. (2011).

Krieg & Mohseni (2013). An orifice nozzle, which consists of a flat plate with a central circular orifice, creates a jet flow with radially converging streamlines; whereas, a cylindrical tube nozzle creates a nearly parallel jet flow. This study will only consider the orifice nozzle configuration because tube nozzles would extend into the surrounding flow, compromising the low drag vehicle shape. In addition the converging radial velocity generated by an orifice nozzle is observed to result in larger impulse than a parallel jet with identical volume flux Krieg & Mohseni (2012). The thrust generated is equal to the rate at which hydrodynamic impulse, I, is created in the propulsive jet, which is not in general equal to momentum transfer across the jetting area. As is derived by Krieg & Mohseni Krieg & Mohseni (2013), the rate at which hydrodynamic impulse is generated is,

$$\frac{dI}{dt} = \pi \int_0^\infty \left[2u^2 r + u \frac{\partial v}{\partial x} r^2 - v^2 r \right]_{x=x_0} dr \,, \qquad (3)$$

where u and v are the axial and radial velocity corresponding to point $[r, x]^T$ in an axisymmetric coordinate system, respectively. The surface integral is computed over the thruster exit plane. Krieg & Mohseni Krieg & Mohseni (2013) parameterized the axial velocity profile at the exit of multiple nozzle configurations in terms of the single parameter b, and the radial velocity profiles by the parameters $k_1^\star$ and $k_2^\star$. Though we will not go through the details of the parameterization in this paper, it suffices to understand that a low value of b corresponds to a parabolic profile (fully developed pipe flow), and approaches a uniform profile as b approaches infinity. A larger value of $k_1^\star$ corresponds to a flow with a larger radial velocity v relative to the axial velocity scale, and a larger value of $k_2^\star$ corresponds to a larger value of the gradient $\partial v/\partial x$ relative to the axial velocity scale. The scale of the axial velocity is the piston velocity which is defined $u_p = \Omega/\pi R^2$, for a jet with volume flux Ω expelled through a circular area of radius R. Using this parameterization the thrust output can be calculated as,

$$F = \frac{dI}{dt} = \rho \pi u_p^2 R^2 \left(g(b) + \frac{k_2^\star - k_1^{\star 2}}{4} \right) , \qquad (4)$$

and $g(b)$ is a function of Bessel functions defined in Krieg & Mohseni (2013). It was also shown in Krieg & Mohseni (2013) that jets ejected through orifice nozzles generated relatively steady velocity profiles, meaning that b, $k_1^\star$, and $k_2^\star$ can all be considered constants for a given thruster arrangement. Therefore, we will combine these terms under a single coefficient, $C_F = \rho\pi \left(g(b) + \frac{k_2^\star - k_1^{\star 2}}{4} \right)$.

Unlike continuous jet propulsion systems commonly used in recreational watercraft, the thrusters discussed here create a propulsive jet from a finite volume of fluid, and after the pulsation has terminated the internal cavity is refilled through the same opening used for jetting. The period of the entire pulsation cycle is given by T, and the duty cycle, λ, is the ratio of the time spent jetting to the time spent refilling. During the refilling phase the ingested fluid starts at rest in the surrounding fluid environment, and ends at rest inside the thruster cavity so the net momentum transfer to the vehicle, and average thrust during refilling, can be considered zero. It should be noted when the vehicle is in motion there is a net momentum transfer associated with bringing the ingested fluid to the vehicle velocity; however, for all cases it is assumed that the jetting velocity is much larger than the average vehicle velocity $u_p \gg \bar{U}$, so the average refilling thrust is still negligible compared to the jetting thrust.

We will restrict our attention to the case where the jet is expelled with a constant piston velocity for the duration of pulsation making the jetting force constant over the jetting phase, and nugatory over the refilling phase,

$$F(t) = \begin{cases} C_F u_p^2 R^2 & : \quad 0 \le t \le \lambda T \\ 0 & : \quad \lambda T < t \le T \end{cases} . \qquad (5)$$

Though this paper focuses on a specific type of underwater thruster, the analysis is easily adaptable to any unsteady propulsor whose thrust output can be described by a periodic oscillation between binary states (on or off).

2.2 Low Re Vehicle Trajectory

In the low Reynolds number regime the drag coefficient on the vehicle is approximately inversely proportional to Re. We will consider the vehicle to be in a quasi-equilibrium state, and denote the maximum and minimum velocities encountered at the end of the thrusting and coasting phases by U_1 and U_0, respectively. During the jetting phase the vehicle dynamics can be written,

$$\ddot{x} = \frac{C_F u_p^2 R^2}{m} - \frac{C_V}{m} \dot{x} \,, \qquad (6)$$

where C_V is a coefficient which is vehicle specific, $C_V = 5\rho S \nu / d$. Using the initial condition which flows naturally from the quasi-equilibrium conditions, $\dot{x}(0) = U_0$, the analytical solution of (6) is,

$$\dot{x}(t) = U_0 e^{-\frac{C_V}{m} t} + \frac{C_F u_p^2 R^2}{C_V} \left(1 - e^{-\frac{C_V}{m} t} \right) . \qquad (7)$$

During the coasting phase the governing vehicle equation is the same as (6) with the thruster forcing term removed. Solving this equation with the final condition $\dot{x}(T) = U_0$ provides the vehicle trajectory during the coasting phase,

$$\dot{x}(t) = U_0 e^{\frac{C_V}{m} T(1-\lambda)} \,. \qquad (8)$$

Finally, imposing the condition that both velocities are equal to U_1 and eachother at $t = \lambda T$ allows the velocity extrema, U_0 and U_1, to be solved in terms of the thruster and vehicle characteristic parameters, the pulsation period,

and duty cycle.

$$U_0 = \frac{C_F u_p^2 R^2}{C_V} \frac{e^{-\frac{C_V}{m}\lambda T} - 1}{e^{-\frac{C_V}{m}T} - 1}\,, \tag{9a}$$

$$U_1 = \frac{C_F u_p^2 R^2}{C_V} \frac{e^{-\frac{C_V}{m}T} - e^{-\frac{C_V}{m}T(1-\lambda)}}{e^{-\frac{C_V}{m}T} - 1}\,, \tag{9b}$$

and the vehicle trajectory is,

$$\dot{x}(t) = \frac{C_F u_p^2 R^2}{C_V} \begin{cases} 1 + e^{-\frac{C_V}{m}t} A & : \quad [0 : \lambda T] \\ e^{\frac{C_V}{m}T - t} B & : \quad [\lambda T : T] \end{cases}\,, \tag{10a}$$

where,

$$A = \frac{e^{\frac{C_V}{m}\lambda T} - e^{\frac{C_V}{m}T}}{e^{\frac{C_V}{m}T} - 1}\,, \text{ and } B = \frac{e^{\frac{C_V}{m}\lambda T} - 1}{e^{\frac{C_V}{m}T} - 1}\,. \tag{10b}$$

Now the velocity of the vehicle can be given at any time in terms of the thruster/vehicle parameters, the pulsation period, and duty cycle.

3 PROPULSIVE EFFICIENCY CALCULATIONS

Propulsive efficiency is defined as the ratio of useful propulsive work done on a vehicle, W_{prop}, to the total energy, or shaft work, W_S, required to generate the propulsion,

$$\eta_P = \frac{W_{\text{prop}}}{W_S}\,. \tag{11}$$

This section defines both of these quantities in terms of the pulsation period, T, and duty cycle, λ.

3.1 Useful Propulsive Work

Useful propulsive work is the integral of the propulsive force over the vehicle trajectory, which by change of variables is the integral of the product of force and velocity over the pulsation time,

$$W_{\text{prop}} = \int_{x(0)}^{x(\lambda T)} F(x)\,dx = \int_0^{\lambda T} F(t)\dot{x}\,dt\,. \tag{12}$$

Since both the thruster force and vehicle velocity are known functions of time, equations (5) and (10) defined respectively in the previous section, the propulsive work can be calculated directly,

$$W_{prop} = \frac{C_F^2 u_p^4 R^4}{C_V}\left[\lambda T - \frac{m}{C_V}\frac{C}{e^{\frac{C_V}{m}T} - 1}\right]\,, \tag{13a}$$

where,

$$C = 1 - e^{\frac{C_V}{m}\lambda T} - e^{\frac{C_V}{m}T(1-\lambda)} + e^{\frac{C_V}{m}T}\,. \tag{13b}$$

3.2 Total Energy Expenditure

The energy required to generate the propulsion is the sum of the shaft work spent jetting, W_{SJ}, and the shaft work spent refilling, W_{SR}. The rate at which work must be applied during jetting was also derived by Krieg & Mohseni Krieg & Mohseni (2013), for the same velocity parameterization as was used to describe the thruster force,

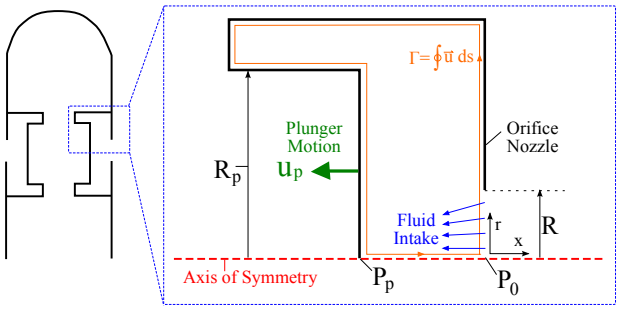

Figure 4: Schematic diagram of the internal thruster geometry and driving mechanism

$$\dot{W}_{SJ} = \frac{dE}{dt} = \frac{\rho\pi}{2} u_p^3 R^2 \left(h(b) + \frac{k_2^\star}{2}\right)\,, \tag{14}$$

where $h(b)$ is another function reported in Krieg & Mohseni (2013). Taking the constant piston velocity into account, the total shaft work exhausted during jetting is, $W_{SJ} = \dot{W}_{SJ}\lambda T$.

During the refill phase the thruster must ingest the same volume of fluid that is ejected during the jetting phase. Assuming that the volume flux is constant during this period as well, then the piston velocity required for refilling is $u_p(\text{refill}) = -u_p \frac{\lambda}{1-\lambda}$. The net momentum transfer during refilling is equal to zero because, in general, fluid at rest outside the thruster cavity is drawn into the cavity, and then returned to a zero momentum state. Though this is not exactly the case when the thruster creates a jet with a stroke ratio above the formation number Krieg & Mohseni (2008), we will limit our analysis to cases where the stroke ratio is at or below the formation number. However, the energy spent refilling as well as the final kinetic energy of the fluid within the cavity is not equal to zero during the refilling phase. Calculating the energy spent refilling requires a knowledge of the pressure on the moving plunger surface, as will be shown later in this derivation. We will derive this pressure first.

Consider the fluid domain internal to the thruster cavity as depicted in Figure 4. The axis of symmetry is by definition a streamline for axisymmetric flows, meaning that the velocity along this line can be described by a velocity potential, $u(0,x) = \partial\phi/\partial x$. From Bernoulli's equation we can equate the pressure on the plunger/piston surface, P_p, to the pressure at the nozzle outlet, P_0,

$$\frac{\partial\phi_p}{\partial t} + \frac{1}{2}u_p^2 + P_p = \frac{\partial\phi_0}{\partial t} + \frac{1}{2}u_0^2 + P_0\,. \tag{15}$$

Integrating the definition of the velocity potential allows us to relate the velocity potentials at the plunger and nozzle

locations by a velocity line integral, $\phi_p = \phi_0 - \int_{x_p}^{0} u\,dx$. Though the velocity along the axis of symmetry is difficult to determine explicitly, the velocity integral is contained in the cavity circulation. The circulation in the thruster cavity is defined as the closed loop velocity integral around the area (see Figure 4), which is just $\Gamma_{cav} = \int_{x_p}^{0} u\,dx + \int_{0}^{R} v\,dr$ since the fluid velocity is zero along all of the cavity surfaces. Taking both of these relations into account in (15) allows the pressure on the plunger to be determined from cavity circulation and characteristic velocities,

$$P_p = P_0 + \frac{1}{2}u_0^2 - \frac{1}{2}u_p^2 + \frac{\partial \Gamma_{cav}}{\partial t} + \int_0^R \frac{\partial v}{\partial t}\,dr\,. \quad (16)$$

The rate at which circulation is generated in the cavity is equal to the flux of vorticity across the nozzle plane,

$$\frac{\partial \Gamma_{cav}}{\partial t} = -\frac{1}{2}u_0^2 - \int_0^R u\frac{\partial v}{\partial x}\,dr\,. \quad (17)$$

Finally an equation for the pressure on the plunger face is realized by inserting this relation into (16),

$$P_p = P_0 - \frac{1}{2}u_p^2 + \int_0^R \left[\frac{\partial v}{\partial t} - u\frac{\partial v}{\partial x}\right]_{x=0} dr\,. \quad (18)$$

If the circulation of the fluid is unaffected by the refill phase, which is a reasonable assumption since we are only considering jets below the formation number, then it follows from the derivation in Krieg & Mohseni (2013) that the nozzle exit plane pressure at the centerline, P_0, is equal to the stagnation pressure, P_∞. Furthermore since there is no radial velocity at the surface of the plunger the pressure is constant over the entire plunger face.

The shaft work required during the refill phase is equal to the rate of change of kinetic energy in the cavity (again assuming that the refilling does not affect the kinetic energy of the external fluid). Since the cavity volume involves a moving boundary Reynolds transport theorem is used to calculate the rate of change of volume energy,

$$\frac{1}{\rho}\frac{dE}{dt} = \int_{cav} \frac{\partial}{\partial t}\left(\frac{1}{2}\vec{u}^2\right) dV + \int_{\delta cav} \vec{u}_b\cdot\vec{n}\frac{1}{2}\vec{u}^2\,dS\,, \quad (19)$$

where $\vec{u}_b$ is the velocity of the boundary, $\vec{n}$ is the boundary surface normal, the first integral term is a volume integral taken over the entire thruster cavity volume, and the second is a surface integral over the cavity boundaries. Assuming inviscid incompressible fluid allows the volume integral to be reduced to a surface integral involving the fluid velocity and the pressure Lamb (1945); Landau & Lifshitz (1959),

$$\frac{1}{\rho}\frac{dE}{dt} = \int_{\delta cav}\left(\frac{1}{2}\vec{u}^2 + P\right)\vec{u}\cdot\vec{n}\,dS + \int_{\delta cav}\vec{u}_b\cdot\vec{n}\frac{1}{2}\vec{u}^2\,dS\,. \quad (20)$$

Since the only moving boundary is the plunger face, and the fluid on that boundary is moving with the same velocity, the flux terms cancel with the moving boundary terms here and we are left with a pressure integral along the plunger boundary and a typical flux integral along the nozzle exit boundary,

$$\frac{1}{\rho}\frac{dE}{dt} = \int_0^R 2\pi r\left[\left(\frac{1}{2}u^2 + \frac{1}{2}v^2 + P(r)\right)u\right]_{x=0} dr + \int_0^{R_p} 2\pi r P_p u_p\,dr\,. \quad (21)$$

The plunger surface pressure, P_p, is given by 18, and the pressure at the nozzle exit boundary ($x = 0$) can be found by integrating the momentum equation in the radial direction, starting from stagnation pressure on the centerline, $P(r,0) = P_0 - \int_0^r u\frac{\partial v}{\partial x} + \frac{\partial v}{\partial t}\,d\varpi - \frac{1}{2}v(r)^2$, where ϖ is just a dummy variable in the radial direction. Using these values for the pressure terms and the same velocity parameterization at the nozzle exit plane that was used to characterize the jet energy, then the rate of work being done during refilling is defined,

$$\dot{W}_{SR} = \frac{\rho\pi}{2}u_p^3\frac{\lambda^3}{(1-\lambda)^3}R^2\left[h(b) + \frac{3k_2^\star}{2} + \frac{R^4}{R_p^4}\right] \quad (22)$$

It should be noted that the kinetic energy of the fluid within the cavity will be decreased significantly due to viscous interactions at the cavity surfaces throughout refilling. However, since this loss in fluid energy is dissipated rather than being returned to the plunger mechanism, this will have no effect on the shaft work required to move the fluid which can be calculated from the kinetic energy of inviscid cavity fluid.

Putting the shaft work during jetting and the shaft work during refilling together and assuming that the velocity parameters b and $k_2^\star$ are identical for jetting and refilling, we arrive at an expression for the total shaft work required for an entire pulsation cycle,

$$W_S = \frac{\rho\pi}{2}u_p^3R^2T\left[\begin{array}{l} h(b)\left(\lambda + \dfrac{\lambda^3}{(1-\lambda)^2}\right) \\ +\dfrac{k_2^\star}{2}\left(\lambda + \dfrac{3\lambda^3}{(1-\lambda)^2}\right) + \dfrac{R^4}{R_p^4}\dfrac{\lambda^3}{(1-\lambda)^2}\end{array}\right]. \quad (23)$$

4 RESULTS

In order to examine the effect of unsteady propulsor duty cycle on propulsive efficiency we consider cases with identical vehicle and thruster parameters (C_V, C_F, and C_E) as well as identical periods of pulsation cycle. For these cases we also want to guarantee that the vehicle travels the same distance over the entire cycle independent of duty cycle, which means that the piston velocity must be increased for the low duty cycle cases by the amount $u_p = u_{p0}\,[1/\lambda]^{1/2}$. u_{p0} is the piston velocity of the case where the jet is expelled for the entire period and the vehicle velocity is constant ($\lambda = 1$). Using these values for piston velocity, and typical values for vehicle and thruster parameters characterized in Krieg & Mohseni (2013, 2008); Krieg et al.

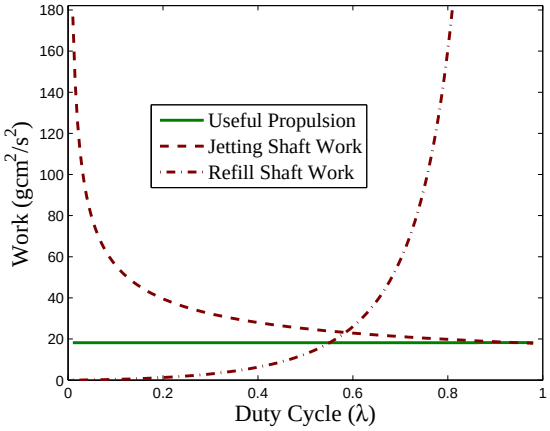

Figure 5: Useful propulsive work done on the vehicle as well as the total energy spent jetting and refilling, while maintaining total distance traveled in a pulsation cycle.

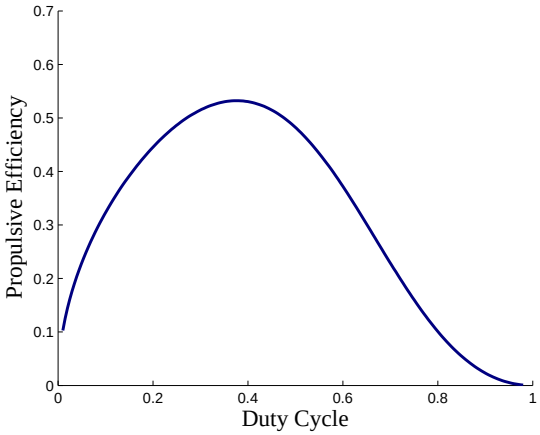

Figure 6: Propulsive efficiency plotted with respect to the duty-cycle, while maintaining total distance traveled in a pulsation cycle.

(2011), the propulsive work and total work done are calculated for the entire range of duty cycles.

It is expected that the propulsive work done on the vehicle is identical for the entire range of duty cycle, since the vehicle travels the same distance over the same period of time for all cases. This is the case as is shown in Figure 5. This figure also shows the shaft work required during both jetting and refilling. Since the useful propulsive work is identical for all cases, the propulsive efficiency will be maximized when the total energy expenditure is minimized, which is the sum of the shaft work spent jetting and the shaft work spent refilling. The shaft work required for jetting decreases with increasing duty cycle, but the shaft work required to refill the cavity grows with increasing duty cycle, suggesting that the total energy expenditure should have a local minimum over the duty cycle range, which will result in a maximum propulsive efficiency.

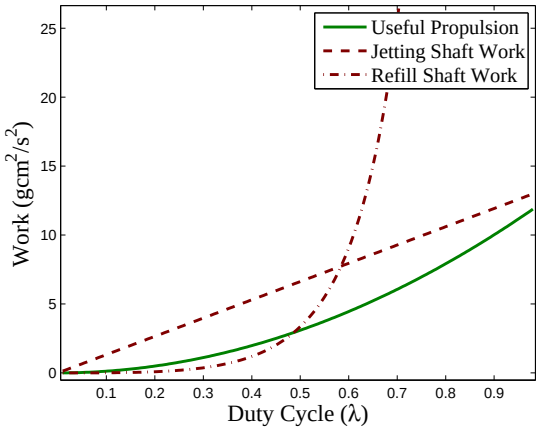

Figure 7: Useful propulsive work done on the vehicle as well as the total energy spent jetting and refilling, while holding thruster force constant.

Figure 6 shows the propulsive efficiency over the range of duty cycle cases, and there is a local maximum at $\lambda = 0.39$ corresponding to the minimum in total energy expenditure. It can be extrapolated from Figures 2 & 5 in Anderson & DeMont (2000) that the squid *Loligo pealei* has a jetting duty cycle of $\lambda = 0.36$ during normal cruising, and increases its duty cycle to $\lambda = 0.5$ during escape jetting. This indicates that during cruising squid alternate between jetting and coasting/refilling with a duty cycle that maximizes propulsive efficiency for quasi-equilibrium swimming. It should be noted that the squid's maximum jetting velocity is limited by the muscular performance in the mantle tissue. During escape jetting, the faster swimming velocity required to move the animal out of harms way can be achieved by increasing the jet velocity and maintaining the optimal duty cycle, but if this is beyond the capability of the squid mantle, then the duty cycle must be increased to increase propulsive output. Instead of maintaining a uniform propulsive output, we can look at the effect of changing duty cycle with a constant piston velocity (corresponding to the maximum thrust output).

Figure 7 shows the useful propulsive work, shaft work exhausted during jetting, and shaft work spent refilling for the cases where the jetting thrust is held to some constant maximum value, u_{p0}. It can be seen that the propulsive work is no longer constant, and exponentially increases with duty cycle, since increasing duty cycle not only increases the total impulse transfer, but also decreases the time spent coasting where kinetic energy is lost to drag forces. The energy spent jetting increases linearly and the energy spent refilling is very similar to the previous cases. Figure 8 shows the propulsive efficiency for the case of constant jetting thrust, and it can be seen that taking this maximum jet velocity into account results in a slightly lower maximum propulsive efficiency which occurs at a higher duty-cycle $\lambda = 0.44$.

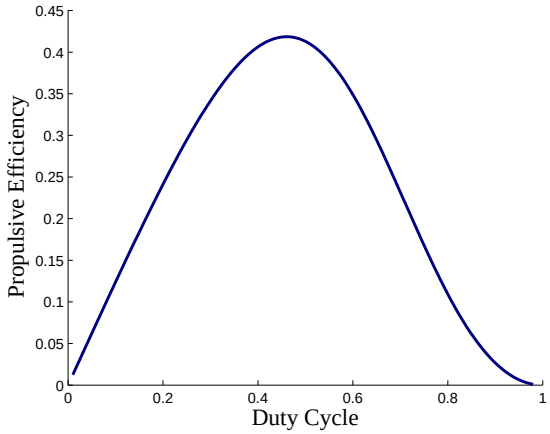

Figure 8: Propulsive efficiency plotted with respect to the duty-cycle, while holding thruster force constant.

CONCLUSIONS

The propulsive efficiency of a vehicle being driven by a periodic application of force is characterized as it relates to forcing duty cycle. It is observed that for an unbounded force the duty cycle which maximizes propulsive efficiency is $\lambda = 0.39$, which is very close to the duty cycle seen in steadily swimming squid. If the forcing is bounded by some maximum value, the optimal duty cycle is shifted higher and corresponds to a lower overall efficiency. This explains the higher duty cycle seen in squid during escape jetting. This derivation requires that the vehicle trajectory be solved analytically which was done for low Re swimming. Future studies will expand this analysis to higher Re swimming.

REFERENCES

Alexander, R. M., 1968. Animal Mechanics. University of Washington Press, Seattle WA.

Anderson, E. & DeMont, E., 2000. 'The mechanics of locomotion in the squid *Loligo pealei*: Locomotory function and unsteady hydrodynamics of the jet and intramantle pressure'. J. Exp. Biol., **203**, pp. 2851–2863.

Bartol, I., Krueger, P., Stewart, W. & Thompson, J., 2009. 'Hydrodynamics of pulsed jetting in juvenile and adult brief squid *Lolliguncula brevis*: evidence of multiple jet 'modes' and their implications for propulsive efficiency'. J. Exp. Biol., pp. 1189–1903. Doi:10.1093/icb/icn043.

Bartol, I., Krueger, P., Thompson, J. & Stewart, W., 2008. 'Swimming dynamics and propulsive efficiency of squids throughout ontogeny'. Integrative and Comparative Biology, **48**(6), pp. 1–14. Doi:10.1093/icb/icn043.

Clark, T., Klein, P., Lake, G., Lawrence-Simon, S., Moore, J., Rhea-Carver, B., Sotola, M., Wilson, S., Wolfskill, C. & Wu, A., 2009. 'KRAKEN: Kinematically roving autonomously kontrolled electro-nautic'. AIAA Aerospace Sciences Meeting. Orlando, Florida.

Fossen, T. I., 1991. Nonlinear modelling and control of underwater vehicles. Ph.D. thesis, Norwegian Institute of Technology, Trondheim, Norway.

Krieg, M., Klein, P., Hodgkinson, R. & Mohseni, K., 2011. 'A Hybrid class underwater vehicle: bioinspired propulsion, embedded system, and acoustic communication and localization system'. Marine Technology Society Journal: Special Edition on Biomimetics and Marine Technology, **45**(4), pp. 153 – 164.

Krieg, M. & Mohseni, K., 2008. 'Thrust Characterization of Pulsatile Vortex Ring Generators for Locomotion of Underwater Robots'. IEEE J. Oceanic Engineering, **33**(2), pp. 123–132.

Krieg, M. & Mohseni, K., 2010. 'Dynamic modeling and control of biologically inspired vortex ring thrusters for underwater robot locomotion'. IEEE Trans. Robotics, **26**(3), pp. 542–554.

Krieg, M. & Mohseni, K., 2012. 'Enhanced impulse of a jet thruster due to radial velocity at the nozzle'. 50th AIAA Sciences meeting including the New Horizons forum and Aerospace Exhibition. Nashville ,TN.

Krieg, M. & Mohseni, K., 2013. 'Modelling circulation, impulse, and kinetic energy of starting jets with non-zero radial velocity'. J. Fluid Mech., **Accepted**.

Krieg, M., Pitty, A., Salehi, M. & Mohseni, K., 2005. 'Optimal Thrust Characteristics of a Synthetic Jet Actuator for Application in Low Speed Maneuvering of Underwater Vehicles'. Proceedings of the OCEANS 2005. MTS/IEEE, Washington, D.C.

Lamb, H., 1945. Hydrodynamics. Dover, New York.

Landau, L. & Lifshitz, E., 1959. Fluid Mechanics, chap. 1.6 Ideal Fluids (Energy Flux). Course of Theoretical Physics (vol.6). Butterworth-Heinemann, Oxford, pp. 9–10.

Lighthill, M., 1975. Mathematical biofluid dynamics. SIAM, Philadelphia.

Mclean, M., 1991. Dynamic performance of small diameter tunnel thrusters. Ph.D. thesis, Naval Postgraduate School, Monterey, California.

Mohseni, K., 2004. 'Pulsatile Jets for unmanned underwater maneuvering'. AIAA paper 2004-6386, Chicago, Illinois. 3rd AIAA Unmanned Unlimited Technical Conference, Workshop and Exhibit.

Mohseni, K., 2006. 'Pulsatile vortex generators for low-speed maneuvering of small underwater vehicles'. Ocean Engineering, **33**(16), pp. 2209–2223.

Vogel, S., 2003. Comparative biomechanics: Life's physical world. Princeton University Press, Princeton, NJ.

Yoerger, D., Cooke, J. & Slotine, J.-J., 1990. 'The influence of thruster dynamics on Underwater Vehicle Behavior and their incorporation into control system design'. IEEE Journal of Oceanic Engineering, **15**(3), pp. 167–178.